Published in final edited form as:
Neurobiol Dis. 2012 January ; 45(1): 479–487. doi:10.1016/j.nbd.2011.08.035.

Effects of aromatase inhibition versus gonadectomy on hippocampal complex amyloid pathology in triple transgenic mice

Cassia R. Overk[1], **Pei-Yi Lu**[2], **Yue-Ting Wang**[2], **Jaewoo Choi**[2], **James W. Shaw**[3], **Gregory R. Thatcher**[2], and **Elliott J. Mufson**[1]

[1]Department of Neurological Sciences, Rush University Medical Center Chicago, IL 60612 USA

[2]Department of Medicinal Chemistry and Pharmacognosy, University of Illinois at Chicago, Chicago, IL 60612

[3]Department of Pharmacy Administration, University of Illinois at Chicago, Chicago, IL 60612

Abstract

Alzheimer's disease (AD) is the most common form of dementia among the elderly with women exhibiting a higher risk than men for the disease. Due to these gender differences, there is great interest in the role that estrogens play in cognitive impairment and the onset of the classic amyloid and tau lesions in AD. Human and rodent studies indicate a strong association between low brain aromatase, sex hormone levels, and beta amyloid deposition. Therefore, the effects of depleting both circulating and brain estrogen levels, through gonadectomy and/or treatment with the aromatase inhibitor, anastrozole, upon hippocampal AD-like pathology in male and female 3xTgAD mice were evaluated. Liquid chromatography-mass spectrometry revealed anastrozole serum levels of 10.19 ng/mL and for the first time brain levels were detected at 4.7 pg/mL. Densitometric analysis of the hippocampus revealed that anastrozole significantly increased $A\beta_{1\text{-}40/42}$- but not APP/Aβ-immunoreactivity in intact 3xTgAD females compared to controls ($p < 0.001$). Moreover, anastrozole significantly increased the number of $A\beta_{1\text{-}40/42}$- compared to APP/Aβ-positive hippocampal CA1 neurons in intact and gonadectomized female mice. Concurrently, anastrozole significantly reduced the APP/Aβ plaque load in 9 months old female 3xTgAD mice. These data suggest that anastrozole treatment differentially affects select amyloid species which in turn may play a role in the extraneuronal to intraneuronal deposition of this peptide.

Introduction

Alzheimer's disease (AD) is the most common form of dementia among the elderly. Although age is a major risk factor for this disease, the relatively rapid decrease in endogenous estrogen levels during menopause (Boyar et al., 1972; Gao et al., 1998) has been attributed to the higher risk for developing AD in women, compared to men (Andersen et al., 1999; Gao et al., 1998; Hy and Keller, 2000; unlisted, 1994). Conversely, males

Address correspondence to: Elliott J. Mufson, Ph.D. Professor of Neurological Sciences, Alla V. and Solomon Jesmer Chair in Aging, Rush University Medical Center, 1735 W. Harrison Street, Suite 300, Chicago, IL 60612, 312-563-3558 tel. 312-563-3571 fax. emufson@rush.edu.

experience a gradual depletion of testosterone that can manifest in dysfunction of androgen-responsive tissues, including the brain (Morley, 2001), and lower serum testosterone levels correlate with increased incidence of AD in men but not women (Hogervorst et al., 2001). The mechanism(s) underlying the role that sex hormones play in the development of AD remain unclear.

The hippocampus is selectively vulnerable in AD (Braak et al., 2006; Braak and Braak, 1991), is responsive to estrogen (Weiland et al., 1997), and is sensitive to both natural fluctuations in circulating (Woolley et al., 1990) as well as experimentally-manipulated estrogen depletion (Gould et al., 1990; Woolley and McEwen, 1992; Woolley and McEwen, 1993; Woolley et al., 1996). Recent evidence suggests that hormone manipulation alters the development of the classic AD neuropathologic lesions, intraneuronal beta amyloid (Aβ) and hyperphosphorylated tau, within the hippocampus in transgenic mouse models of this disease (Carroll et al., 2007; Carroll et al., 2010; Rosario et al., 2010; Rosario et al., 2006). Aromatase, which converts androgens to estrogens, may also contribute to amyloid deposition.

Aromatase is a member of the CYP450 superfamily and is found in the ovaries, adrenal glands, adipose tissues and brain. During menopause, the primary source of estrogen switches from ovarian, for systemic distribution, to tissue-specific synthesis for local effects (Grodin et al., 1973), which are independent of circulating levels of sex steroids (Mukai et al., 2010). Recent studies evaluated local brain hormone and serum levels in non-demented and demented individuals (Yue et al., 2005), which identified region-specific changes in brain aromatase (Ishunina et al., 2005). These data indicate a negative correlation between brain aromatase mRNA levels and plaque density in male and female AD patients (Yue et al., 2005). While the functional consequences of brain aromatase remain unknown, many women with breast cancer have been treated with aromatase inhibitors (AIs) (Howell, 2006). Although a few small clinical trials suggest that AI's produce a decline in verbal and visual learning and memory (Bender et al., 2007; Castellon et al., 2004), larger trials found no cognitive impairments between the tested groups (Jenkins et al., 2008).

Animal models of AD were employed to determine the interaction that androgens, estrogens, and aromatase have upon the development of AD-like pathology. Of particular interest is the finding that crossing an APP_{swe} single transgenic with an aromatase knock-out mouse increased amyloid plaque density (Yue et al., 2005). Moreover, gonadectomy (GDX) increased $A\beta_{1\text{-}40/42}$ load and intraneuronal tau in the hippocampus of 6-7 month old male (Rosario et al., 2006) and female (Carroll et al., 2007) triple transgenic (3xTg-AD) mice. These findings suggest that both brain and circulating estrogen play a crucial role in the expression of AD pathology. Therefore, we investigated the effect of anastrozole, an AI, in the presence and absence of circulating hormones on AD-like pathology in 3xTg-AD mice.

Materials and Methods

Subjects

A colony of 3xTgAD mice (Oddo et al., 2003) was generated from breeding pairs provided by Dr. F. LaFerla, University of California Irvine. Mice were housed in plastic cages, given ad libitum access to food and maintained on a 12:12-hour light:dark cycle. All animal care and procedures were conducted with approved institutional animal care protocols and in accordance with the NIH Guide for the Care and use of Laboratory Animals.

Surgery

All mice were anaesthetized with ketamine/xylazine (95 and 5 mg/kg body weight, respectively) prior to GDX at 3 months of age except the female intact groups (Table 1). In

females, a dorsal midline incision was made, the muscle wall was pierced with forceps, and the ovaries were clamped and ligated to the level of the fallopian tube. Testes were removed by creating incisions in the scrotum and tunica of the first testicle. The testis, van deferens, and the attached testicular fat pad were exteriorized, blood vessels were clamped and tied off. All incisions were closed using wound clips. Groups treated with hormone pellets (InnovativeResearch of America, FL) were implanted subcutaneously between the scapulas. Pellets released hormone treatment (HT) over 90 days and were replaced at 6 months of age, and consisted of 17β-estradiol (0.25 mg) and progesterone (25 mg) or 12.5 mg testosterone for females and males, respectively.

Diet and Anastrozole Treatment

All groups were placed on Teklad Global Soy Protein-free diet to minimize exposure to phytoestrogens (Teklad 2020x, Harlan laboratories, Madison WI). Oral consumption of the aromatase inhibitor anastrozole is hampered by poor drug palatability when added to drinking water. To overcome this issue, we developed a novel oral delivery technique for anastrozole mixed in a solid hydration gel matrix, which functions as a replacement for water (Overk et al., 2011). Briefly, anastrozole powder (45 mg, AstraZeneca, UK) was mixed with red food coloring (40 μL, McCormick; Sparks, MD) and propylene glycol (1 mL, Fisher Scientific; Pittsburg, PA) on a glass slide forming a slurry, which was then transferred to a heated bag of no-sugar-added banana-flavored hydration gel (8 oz LabGel; ~236 mL; ClearH2O; Portland, ME). The bag was closed and vigorously shaken until the red-dyed anastrozole was homogenously dispersed throughout the bag. The gel was immediately transferred to the gel delivery device, as described previously (Overk et al., 2011). Data from our previous study demonstrated that animals consumed approximately 2.0 mL of gel/day, which equates to an anastrozole dose of approximately 0.4 mg/animal/day (Overk et al., 2011). Vehicle gel was prepared in the same manner with the exception of the drug and half the amount of food dye so that the investigator could distinguish anastrozole-containing gel from vehicle gel. Gel consumption and body weights were recorded periodically throughout the week.

Tissue collection—At 9 months of age, mice were deeply anaesthetized with ketamine/xylazine (95 and 5 mg/kg body weight, respectively) and cardiac blood was collected just prior to transcardial perfusion with cold physiological saline (pH 7.4). Brains were removed from the calvarium and hemisected; one hemisphere was placed in 4% paraformaldehyde and 0.1% glutaraldehyde in 0.1 M phosphate-buffered saline (PBS; pH 7.4) fixative for 24 h, cryoprotected in 30 % sucrose in PBS at 4 °C for at least 24 h and coronal hemisections were cut frozen on a sliding knife microtome at 40 μm thickness into six adjacent series and stored at −20 °C in a cryoprotectant solution (30 % ethylene glycol, 30 % glycerol, in 0.1 M PBS) prior to processing. The other hemisphere was dissected on ice into discrete neuroanatomical regions and frozen on dry ice.

Immunohistochemistry

Free-floating sections were immunohistochemically processed using antibodies directed against APP/Aβ (6E10; Covance, NJ; 1:2000) (Overk et al., 2009) or soaked in a solution of 99% formic acid for 5 minutes followed by boric acid neutrizilation (0.1M; pH 8.5) prior to incubation with an antibody directed against $A\beta_{1\text{-}40/42}$ (1:300; Zymed 71-5800; CA) (Rosario et al., 2006), incubated in the Vectastain ABC kit (Vector Labs, CA), and visualized using diaminobenzidine (DAB, Sigma, St Louis, IL). Immunohistochemical controls for APP/Aβ, included primary antibody deletion, which revealed immunonegativity (Overk et al., 2009). To determine whether formic acid pretreatment of tissue used with antibodies directed against $A\beta_{1\text{-}40/42}$ altered the staining APP/Aβ immunoreactivity, sections were treated with and without 99% formic acid following the same protocol used with the

$A\beta_{1\text{-}40/42}$ prior to immunolabeling with the APP/Aβ antibody. Formic acid did not change the number of labeled neurons but instead increased the cellular staining intensity (Supplementary Fig. 1).

Densitometry

Quantification of the relative optical density (OD) of Aβ/APP- (Fig. 1A) and $A\beta_{1\text{-}40/42}$-immunoreactive (ir) CA1 pyramidal neurons (Fig. 1B,C) was performed using the densitometry software program Image 1.60 (Scion, Frederick, MD) as reported previously (Jaffar et al., 2001; Ma et al., 1999; Mufson et al., 1997; Perez et al., 2005). Anatomical nomenclature was based on the atlas of Paxinos and Franklin (Paxinos and Franklin, 2001). Every sixth section (separated by 240 μm) was analyzed using a 40× objective and centering the camera over the pyramidal layer of the CA1 field. The first captured frame marked the division between the end of the region inferior (CA2/3) and the start of region superior (CA1). Progressing from CA1 to the subiculum, the first three adjacent but non-overlapping fields were outlined manually. The OD and area measurements were automatically analyzed in gray-scale images, using the computer program. Previous studies have shown that OD measurements reflect changes in protein expression parallel those obtained using a biochemical protein assay (Mufson et al., 1997).

Stereology Procedure

Optical Fractionator—Stereological methods were used to estimate the number of hippocampal CA1 pyramidal neurons that were immunoreactive for APP/Aβ and $A\beta_{1\text{-}40/42}$ utilizing an unbiased optical fractionator sampling design (Jaffar et al., 2001; Overk et al., 2009; Perez et al., 2005). Immunoreactive neurons were only counted if the first recognizable profile came into focus within the counting frame. This method allowed for a uniform, systematic, and random design. Focusing through the Z-axis revealed that the APP/Aβ and $A\beta_{1\text{-}40/42}$ antibodies penetrated the full depth of each section. Section thickness was determined at each site by focusing on the top of the section, zeroing the z-axis and focusing on the bottom of the section. The dissector height was based on section thickness for each case with a 1μm top and bottom guard zone. The forbidden zones were never included in the cell counting.

Microscopic evaluation $A\beta_{1\text{-}40/42}$ APP/Aβ-ir revealed a granular particulate with no clear cellular demarcation (Fig. 1C) making it difficult to apply stereological counting methods within the hippocampus. To overcome this caveat, following initial OD measurements, coverslips were removed, and the tissue was defatted in chloroform and alcohol (50:50 v/v) and stained for Nissl substance using a standard protocol (Hof et al., 1995) to more precisely visualize the $A\beta_{1\text{-}40/42}$-ir within neurons (Fig 1D). Optical fractionator parameters for estimating the number of $A\beta_{1\text{-}40/42}$-positive hippocampal CA1 neurons in male mice were as follows: perikarya within sections separated by approximately 240 μm were outlined using a 10× objective attached to a Nikon Optihot-2 microscope. A systematic sampling of the outlined areas was made from a random starting point using StereoInvestigator 8.21.1 software (Micro-BrightField, Cochester, VT). Counts were taken at predetermined intervals (x = 101, y = 161), and a counting frame (30 × 30 μm = 900 μm^2) was superimposed on the live image of the tissue sections. Sections were analyzed using a 60 × 1.4 PlanApo oil immersion objective with a 1.4 numerical aperture. The average Gunderson coefficient of error, m = 1 (Gundersen et al., 1999), was 0.065 ± 0.0006. Based on a pilot study, we determined that for females a sampling grid size of × = 161, y = 161 and a sampling of every 12^{th} hippocampal section (480 μm) was appropriate with an average coefficient of error of was 0.081 ± 0.008. Average section thickness across groups was 10 μm.

Unlike $A\beta_{1\text{-}40/42}$ staining, APP/Aβ-ir was clearly visualized within a labeled neuron; therefore Nissl counterstaining was not required. Hippocampal CA1 neurons were counted in every 12^{th} section (480 μm) using a counting frame (30 × 30 μm = 900 μm^2) and sampling grid size (x= 166, y = 114) for both males and females. The average coefficient of error was 0.09 ± 0.01 with an average tissue thickness of 8.8 μm.

Plaque Area Fraction Fractionator—The subiculum was outlined in sections 240 μm apart extending from its dorsal-rostral location to its more ventral-caudal portion. Subicular $A\beta_{1\text{-}40/42}$- and APP/Aβ-ir plaques (Fig. 1E, E', E") were evaluated using a counting frame of 140 × 90 μm, a sampling grid (x = 155, y = 155), and a grid space of 7 μm.

Serum and Brain Anastrozole Levels—Quantification of anastrozole from serum was corrected for a five-fold dilution that occurred during the extraction of 10 μL serum volume into a final volume of 50 μL as previously described (Overk et al., 2011). Brain anastrozole levels were similarly quantified with the aid of liquid chromatography-tandem mass spectrometry (LC-MS/MS) using a modification of the serum extraction method (Overk et al., 2011; Yu et al., 2011), and samples were run in duplicate. Solvent-resistant pipette tips with charcoal filters (Molecular BioProducts, San Diego CA) were used for all procedures involving solvents. Briefly, ice-cold high performance liquid chromatography (HPLC)-grade methanol was added to duplicate brain samples (1mL/100 mg). Samples were spiked with 50 ng/mL internal standard (10 μL), ground twice with a hand held homogenizer, and centrifuged at 4 °C for 15 minutes at 14,000 rpm (Eppendorf 5810R; Hamburg, Germany). The supernatant was transferred to a clean tube and evaporated to dryness under nitrogen. The dried samples were reconstituted with HPLC-grade acetonitrile: water (100 μL; 50:50, v/v) containing 0.1% formic acid, vortexed for 10 s, and centrifuged (14,000 rpm). The clear supernatant was transferred to a sample vial (Waters; Milford, MA) and analyzed using LC-MS/MS. Brain anastrozole levels were corrected for the variation in brain mass. Brain weight was converted into mL brain tissue using the specific gravity for mouse brain (1.05) (Nelson et al., 1971) and the density of water (1 mg/mL).

Calibration standard and quality control—Stock solutions (1 mg/mL) of anastrozole (AstraZeneca, England) and verapamil (US Pharmacopeia, Rockville MD) were dissolved in acetonitrile: water (50:50, v/v) and stored at −20 °C. Duplicate anastrozole calibration curves were prepared by spiking blank brain tissue with verapamil (10 μL; 50 ng/mL) and anastrozole (10 μL) at concentrations of 0.625, 1.25, 2.5, 5, 10, 20 ng/mL and extracting the sample as describe above. Quality control samples of 1.8 and 3.6 ng/mL were prepared using naïve brain tissue; final concentrations were ten-fold more dilute.

Chromatographic conditions—A Waters Alliance 2695 Separation Module was used to resolve each brain extract. Liquid-chromatography was carried out at room temperature on an Xbridge C18 (3.5 μm; 2.1 mm x 100 mm) column (Waters Corporation, Milford, MA). The mobile phase consisted of water with 0.1% formic acid as solvent A and acetonitrile with 0.1% formic acid as solvent B. The compounds were eluted with 70% isocratic solvent B, and the flow rate was 0.2 mL/min. An aliquot (10 μL) of each sample was injected onto the column. Run time was 8 min per sample.

Mass-spectrometric conditions—Mass spectrometric analysis was performed using a Thermo-Finnigan TSQ Quantum triple quadrupole mass spectrometer (West Palm Beach, FL, USA) equipped with an electrospray ionization (ESI) source operating in positive mode. Selected reaction monitoring (SRM) was performed for transitions 294 → 225 and 455 → 165 for anastrozole and the internal standard, respectively. The source temperature was set at 300 °C and the ESI voltage set to 3.5 kV. Collision energy was set to 19 eV and 28 eV for

internal standard and anastrozole, respectively. Scan width was 2.0 atomic mass units and scan time was 1.0 s for each compound.

Data analysis

All statistical analyses were performed using Stata/MP 10.0 (Windows version, Stata Corp LP, College Station, TX) or GraphPad Prism 5 (Windows version, GraphPad Software Inc, San Diego, CA) and with a two-tailed probability of Type I error of 0.05.

Serum and brain concentrations of anastrozole were measured using LC-MS/MS. The ratio of the peak area for anastrozole to the peak area for the internal standard was derived and compared against a sigmoid log dose-response curve to estimate the associated anastrozole concentration. One-way analysis of variance (ANOVA) was used to compare mean serum and brain anastrozole concentrations among groups of subjects classified according to sex and hormonal status. For males, hormonal status was defined as GDX with or without HT, whereas females were classified according to hormonal status as intact or GDX.

A survival analysis was conducted following an HT-related difference in unexplained death among female animals. The Kaplan-Meier estimator was used to compare survivorship (time to sacrifice in days) among groups of subjects classified according to treatment (anastrozole or plain) and hormonal status. Separate analyses were performed for male and female animals. For male animals, hormonal status was defined as GDX with or without HT. Female animals were classified according to hormonal status as intact or GDX with or without HT. The log-rank test compared survival distributions of treatment-by-hormonal-status groups.

Optical density (OD) measurements were converted to average subject-level percentage increases over background using the following formula:

$$\text{Average percentage increase} = 100 \times ((\text{OD}_{\text{sample}} - \text{OD}_{\text{background}})/\text{OD}_{\text{background}}) \quad \text{Eq. 1}$$

Ordinary least squares (OLS) regression was applied to model the resulting percentages as a function of treatment, hormonal status (GDX with or without HT), the interaction of treatment with hormonal status, and section number (i.e., 1, 7, 13, 19, 25, or 31 with each section being separated by 240 μm). A separate model was fit to the data for each sex and antibody type ($A\beta_{1\text{-}40/42}$ or APP/Aβ). When fitting the models, a robust variance estimator was applied to allow for arbitrary within-subject correlation. Estimated means were compared between treatment groups within groups defined by hormonal status. The estimated means of subjects not assigned to anastrozole were also compared between hormonal status groups. The Holm procedure (Holm, 1979) was applied to adjust for multiple comparisons.

Poisson regression was applied to model stereological counts of CA1 pyramidal neurons as a function of treatment, hormonal status, antibody type, and interactions of these three factors. For male animals, hormonal status was defined as GDX with or without HT, whereas female animals were classified according to hormonal status as intact or GDX without HT. Estimated neuronal counts were compared between treatment groups within groups defined according to the interaction of sex, hormonal status, and antibody type. Similarly, estimated counts were compared between antibodies within groups defined by the interaction of sex, hormonal status, and treatment. When fitting the models, a robust variance estimator was applied to allow for arbitrary within-subject correlation. The Holm procedure adjusted for multiple comparisons.

Mean plaque surface area was modeled as a function of treatment, hormonal status (GDX or intact), the interaction of treatment with hormonal status, and age. A separate model was fit to the areas identified using each antibody type. Four subjects were excluded from the analyses because they were not 9 months of age. Plaque surface areas identified using the $A\beta_{1\text{-}40/42}$ antibody were approximately normally distributed; hence, they were modeled using OLS regression. Several deviant cases were observed when analyzing surface areas identified using the APP/Aβ antibody. Because of this, areas visualized using the APP/Aβ antibody were modeled using the minimum scale (S) estimator (Rousseeuw and Leroy, 1987; Rousseeuw and Yohai, 1984), which is robust to bad leverage points. A heteroscedasticity-consistent variance estimator was applied when fitting both models. Estimated mean areas were compared between treatment groups within groups defined according to hormonal status. The difference in treatment-group differences between hormonal-status groups was also evaluated. The Holm procedure was applied to adjust for multiple comparisons.

Results

Survival Analysis

There was a significant difference in survivorship among the groups defined by the interaction of hormonal status and treatment ($p < 0.0001$). Hormone treated female animals had a 50% survival rate at 181 days, while those treated with HT and anastrozole had a median survival rate of 242 days (Fig. 2). Due to the observed association between HT and survivorship, intact female animals were substituted for those treated with HT in all subsequent analyses.

Anastrozole concentrations in serum and brain

Serum and brain concentrations of anastrozole were measured using LC-MS/MS (Fig. 3A). There were no significant differences in mean serum or brain anastrozole concentrations among groups defined according to sex and hormonal status ($p = 0.6257$), and anastrozole was not detected in tissues from vehicle groups. Mean anastrozole concentrations were 10.2 ± 4.8 ng/mL and 4.7 ± 2.7 pg/mL for serum and brain, respectively. Serum and brain anastrozole concentrations were significantly positively correlated (Fig. 3B; $r = 0.79$, $p < 0.0001$).

Body weights

Intact females treated with anastrozole gained weight at a significantly faster rate than females that received the vehicle (data not shown; $p < 0.05$) (Overk et al., 2011).

Densitometry

Pharmacological hormone depletion selectively effected hippocampal CA1 $A\beta_{1\text{-}40/42}$ load in female but not male mice (Fig. 4A). Intact females treated with anastrozole displayed a significant increase in $A\beta_{1\text{-}40/42}$-ir compared to intact females given untreated gel ($p < 0.001$). There was no significant difference between anastrozole-treated and vehicle-treated GDX females or between groups of males. Analysis of APP/Aβ load in the CA1 pyramidal cell layer revealed no significant differences between treatment groups for either sex (Fig. 4B). Since densitometric measurements were performed throughout the rostral caudal extent of the CA1 field, we analyzed the affect of anatomical level upon OD levels. Interestingly, we found a significant increase in OD values moving from rostral to caudal within the CA1 field ($p < 0.05$).

Stereologic Counting

Anastrozole treatment did not affect the number of $A\beta_{1\text{-}40/42}$- or APP/Aβ-positive CA1 neurons (Fig. 5A-C). The number of $A\beta_{1\text{-}40/42}$-positive neurons was significantly larger than the number of APP/Aβ-positive neurons for anastrozole-treated female mice ($p < 0.001$). Conversely, the number of $A\beta_{1\text{-}40/42}$-positive neurons was smaller than the number of APP/Aβ-positive neurons for GDX males that received HT and were not treated with anastrozole ($p = 0.004$).

Plaque Area

The mean area occupied by APP/Aβ-positive plaques was smaller for intact animals treated with anastrozole (Fig. 6A, B) compared to vehicle ($p = 0.005$) (Fig. 6B-F). However, anastrozole treatment had no effect on the mean area occupied by APP/Aβ-positive plaques among GDX animals ($p = 0.29$), and anastrozole treatment had no effect on the area occupied by $A\beta_{1\text{-}40/42}$-positive plaques for intact ($p = 0.12$) or GDX ($p = 0.15$) groups (Fig. 6A).

Discussion

Technical Considerations

Unexpected morbidity occurred, which required animals to be euthanized within the HT female 3xTgAD groups. Surgical complications due to GDX were ruled out since only mice receiving the estrogen and progesterone implant became morbid. Necropsy of the female HT mice revealed infection in the uterine area and in some cases enlarged bladders. These finding are in line with a recent report of unexpected animal deaths due to urine retention and cystitis in mice treated with 17β-estradiol slow release pellets (Pearse et al., 2009). On the other hand, female HT mice receiving anastrozole survived for an additional 60 days, suggesting that decreased production of estrogen from non-ovarian sources significantly prolonged survival rates. Due to this morbidity female, HT groups were replaced with intact females randomized to anastrozole treatment.

Data Commentary

We report for the first time that orally administered anastrozole penetrates the blood brain barrier, and alters $A\beta_{1\text{-}40/42}$ pathology in female but not male 3xTgAD mice. Densitometric analysis revealed that anastrozole significantly increased $A\beta_{1\text{-}40/42}$-ir in 9 month old intact female but had no effect on male 3xTgAD mice. Stereological estimates of the number of CA1 pyramidal neurons revealed a significant increase in $A\beta_{1\text{-}40/42}$- compared to APP/Aβ-positive neurons in transgenic female mice treated with anastrozole. While anastrozole treatment did not affect CA1 neuronal number in males, testosterone in the absence of anastrozole significantly decreased $A\beta_{1\text{-}40/42}$-ir neuron number compared with APP/Aβ-ir in 3xTgAD mice. Evaluation of extraneuronal amyloid plaque area in the subiculum suggested that anastrozole significantly decreased the area occupied by APP/Aβ-ir plaques in female 3xTgAD mice. Taken together, these findings suggest that orally administered anastrozole significantly affects AD-like pathology in female but not male 3xTgAD mice at 9 months of age, further supporting the hypothesis that AD-pathology may be manipulated in a sex-dependent manner. To our knowledge, this is the first report of the detection of anastrozole in the brain, providing evidence that anastrozole, similar to letrozole, another third generation aromatase inhibitor (Goyal et al., 2008; Kil et al., 2009), penetrates the blood brain barrier. Comparisons of brain and serum levels of anastrozole indicate that the brain concentration of anastrozole was 0.05% of the concentration found in serum. While the concentration of anastrozole in brain was below its IC_{50} (Plourde et al., 1994), there were significant effects upon $A\beta_{1\text{-}40/42}$ hippocampal pathology. Increasing the dose of anastrozole

was not feasible as the palatability and therefore ingestion of the hydration gel would have decreased likely resulting in dehydration (Overk et al., 2011).

Densitometry revealed that anastrozole significantly increased the number of hippocampal CA1 $A\beta_{1\text{-}40/42}$-ir neurons in intact females, which is in agreement with reports of increased $A\beta_{1\text{-}40/42}$ plaques in mutant mice resulting from crossing an aromatase knockout mouse with the APP_{swe} transgenic AD mouse model (Yue et al., 2005). There was no significant difference at the 9 mos of age in $A\beta_{1\text{-}40/42}$-ir between the intact and GDX females randomized to control gel. Although there was a trend toward increasing $A\beta_{1\text{-}40/42}$-ir between intact and GDX females, this finding is in contrast to that reported in 7 month old female 3xTgAD mice (Carroll et al., 2007), which may be accounted for by the different ages of the mice used in the two studies. In contrast to females, hormone manipulation in males failed to reveal a significant difference in $A\beta_{1\text{-}40/42}$-ir OD between hormone- or anastrozole-treated groups. On the other hand, there was a non-significant trend toward GDX increasing $A\beta_{1\text{-}40/42}$-ir compared to testosterone-treated mice, which is in contrast a report of a significant increase in $A\beta_{1\text{-}40/42}$-ir OD with GDX compared to HT in male 3xTgAD mice (Rosario et al., 2006). The difference between these finding may be related to type of androgen used in each study. In the present study, testosterone was used since it is aromatized into estrogen, while the earlier study used the non-aromatizable androgen, dihydrotestosterone, which has a greater affinity for the androgen receptor. The present data revealed that aromatase inhibition affected $A\beta_{1\text{-}40/42}$ pathology in the CA1 field of the hippocampus in females, but not males, lending support to the hypothesis that testosterone plays a role in $A\beta_{1\text{-}40/42}$ development in males, while in females aromatized estrogens are a crucial variable that affect the formation of $A\beta_{1\text{-}40/42}$ pathology (Pike et al., 2009).

Unbiased stereology revealed significant differences between the number of APP/Aβ- compared to $A\beta_{1\text{-}40/42}$-positive neurons. It is important to recognize that APP/Aβ recognizes $A\beta_{1\text{-}16}$, while the $A\beta_{1\text{-}40/42}$ antibody was generated against a synthetic 30 amino acid sequence from the C-terminal end of Aβ1-43. While there is minor overlap between the two antibodies at amino acids 13–16, this difference, most likely, does not underlie the quantitative differences identified in the manuscript. In fact, the number of neurons displaying $A\beta_{1\text{-}40/42}$-ir was nearly double that of those positive for APP/Aβ in intact females treated with anastrozole. The number of $A\beta_{1\text{-}40/42}$- compared with APP/Aβ-ir neurons in anastrozole-treated GDX females also increased significantly. These data suggest that anastrozole altered the intraneuronal composition of Aβ peptide recognized by the APP/Aβ compared to $A\beta_{1\text{-}40/42}$ antibody. In HT males, there was a shift toward more APP/Aβ-ir neurons suggesting that testosterone may be neuroprotective in males possibly through a role in $A\beta_{1\text{-}40/42}$ processing. This shift may also be related to the observation that plaque pathology develops at a later age in male than female 3xTgAD mice (Oddo et al., 2003; Oh et al., 2010).

Plaque area was only analyzed in female 9 mos old 3xTgAD mice since males did not display plaques. Anastrozole treatment significantly decreased APP/Aβ plaque area in the subiculum in intact females, while there was a non-significant trend toward reduced area for $A\beta_{1\text{-}40/42}$-ir plaques. The current findings are in contrast to the increased plaque load reported following crossing of a single APP transgenic mouse with an aromatase knockout mouse (Yue et al., 2005). This discrepancy may be due to the different methods used to inhibit aromatase. The present study used ingested AI to create a pharmacological model from 3 to 9 mos of age, while in the earlier study an APP transgenic was crossed with an aromatase knockout mouse, which is more of a model for neuronal developmental events rather than for aging.

To our knowledge this is the first study investigating the effects of anastrozole upon the deposition of AD-like pathology in a transgenic model of AD. These data suggest that anastrozole altered the intra- and extra-neuronal composition of the Aβ peptide recognized by the APP/Aβ and $A\beta_{1\text{-}40/42}$ antibodies in female mice. While the mechanism(s) through which anastrozole differentially effects intra- versus extra-neuronal Aβ remain unknown, there are several possibilities including altering the amino acid sequence recognized by the antibody, altering the ratio of insoluble to soluble Aβ or by affecting Aβ degrading enzymes such as neprilysin and insulin degrading enzyme (IDE), and experiments targeting these mechanisms are underway. Additional studies evaluating both the pathological and cognitive effects of abiraterone, a potent inhibitor of testosterone synthesis (Barrie et al., 1994), and phenytoin, an antiepileptic known to increase androgen metabolism (Meyer et al., 2006), as well as the continued evaluation of aromatase inhibitors at different ages and stages of dementia remain to be investigated. These studies would further add to our understanding the role of peripheral and central sex hormones play in the progression of the clinical pathological sequel of AD.

Supplementary Material

Refer to Web version on PubMed Central for supplementary material.

Acknowledgments

The authors thank AstraZeneca for providing anastrozole and the Rush Proteomics and Biomarkers Core and C. A. Crot of the Mass Spectrometry Laboratory at the University of Illinois at Chicago for serum LCMS studies. This work was supported in part by TGAG000257, AG10688, and Shapiro Foundation to EJM.

References

Andersen K, et al. Gender differences in the incidence of AD and vascular dementia: The EURODEM Studies. EURODEM Incidence Research Group. Neurology. 1999; 53:1992–7. [PubMed: 10599770]

Barrie SE, et al. Pharmacology of novel steroidal inhibitors of cytochrome P450(17) alpha (17 alpha-hydroxylase/C17-20 lyase). J Steroid Biochem Mol Biol. 1994; 50:267–273. [PubMed: 7918112]

Bender CM, et al. Memory impairments with adjuvant anastrozole versus tamoxifen in women with early-stage breast cancer. Menopause. 2007; 14:995–998. [PubMed: 17898668]

Boyar R, et al. Synchronization of augmented luteinizing hormone secretion with sleep during puberty. N Engl J Med. 1972; 287:582–586. [PubMed: 4341276]

Braak H, et al. Staging of Alzheimer disease-associated neurofibrillary pathology using paraffin sections and immunocytochemistry. Acta Neuropathol. 2006; 112:389–404. [PubMed: 16906426]

Braak H, Braak E. Neuropathological stageing of Alzheimer-related changes. Acta Neuropathol. 1991; 82:239–259. [PubMed: 1759558]

Carroll JC, et al. Progesterone and estrogen regulate Alzheimer-like neuropathology in female 3xTg-AD mice. J Neurosci. 2007; 27:13357–13365. [PubMed: 18045930]

Carroll JC, et al. Continuous and cyclic progesterone differentially interact with estradiol in the regulation of Alzheimer-like pathology in female 3xTransgenic-Alzheimer's disease mice. Endocrinology. 2010; 151:2713–2722. [PubMed: 20410196]

Castellon SA, et al. Neurocognitive performance in breast cancer survivors exposed to adjuvant chemotherapy and tamoxifen. J Clin Exp Neuropsychol. 2004; 26:955–969. [PubMed: 15742545]

Gao S, et al. The relationships between age, sex, and the incidence of dementia and Alzheimer disease: a meta-analysis. Arch Gen Psychiatry. 1998; 55:809–815. [PubMed: 9736007]

Gould E, et al. Gonadal steroids regulate dendritic spine density in hippocampal pyramidal cells in adulthood. J Neurosci. 1990; 10:1286–1291. [PubMed: 2329377]

Goyal S, et al. Excellent response to letrozole in brain metastases from breast cancer. Acta Neurochir. 2008; 150:613–4.

Grodin JM, et al. Source of estrogen production in postmenopausal women. J Clin Endocrinol Metab. 1973; 36:207–214. [PubMed: 4688315]

Gundersen HJ, et al. The efficiency of systematic sampling in stereology--reconsidered. J Microsc. 1999; 193:199–211. [PubMed: 10348656]

Hof PR, et al. Human orbitofrontal cortex: cytoarchitecture and quantitative immunohistochemical parcellation. J Comp Neurol. 1995; 359:48–68. [PubMed: 8557847]

Hogervorst E, et al. Serum total testosterone is lower in men with Alzheimer's disease. Neuro Endocrinol Lett. 2001; 22:163–168. [PubMed: 11449190]

Holm S. A simple sequentially rejective multiple test procedure. Scandinavian Journal of Statistics. 1979; 6:65–70.

Howell A. The 'Arimidex', Tamoxifen, Alone or in Combination (ATAC) Trial: a step forward in the treatment of early breast cancer. Rev Recent Clin Trials. 2006; 1:207–215. [PubMed: 18473974]

Hy LX, Keller DM. Prevalence of AD among whites: a summary by levels of severity. Neurology. 2000; 55:198–204. [PubMed: 10908890]

Ishunina TA, et al. Diminished aromatase immunoreactivity in the hypothalamus, but not in the basal forebrain nuclei in Alzheimer's disease. Neurobiol Aging. 2005; 26:173–194. [PubMed: 15582747]

Jaffar S, et al. Neuropathology of mice carrying mutant APP(swe) and/or PS1(M146L) transgenes: alterations in the p75(NTR) cholinergic basal forebrain septohippocampal pathway. Exp Neurol. 2001; 170:227–243. [PubMed: 11476589]

Jenkins VA, et al. Effects of anastrozole on cognitive performance in postmenopausal women: a randomised, double-blind chemoprevention trial (IBIS II). Lancet Oncol. 2008; 9:953–961. [PubMed: 18768369]

Kil KE, et al. Synthesis and PET studies of [(11)C-cyano]letrozole (Femara), an aromatase inhibitor drug. Nucl Med Biol. 2009; 36:215–223. [PubMed: 19217534]

Ma SY, et al. Dopamine transporter-immunoreactive neurons decrease with age in the human substantia nigra. J Comp Neurol. 1999; 409:25–37. [PubMed: 10363709]

Meyer RP, et al. Anti-epileptic drug phenytoin enhances androgen metabolism and androgen receptor expression in murine hippocampus. J Neurochem. 2006; 96:460–472. [PubMed: 16336225]

Morley JE. Androgens and aging. Maturitas. 2001; 38:61–71. [PubMed: 11311591]

Mufson EJ, et al. Reduction in p140-TrkA receptor protein within the nucleus basalis and cortex in Alzheimer's disease. Exp Neurol. 1997; 146:91–103. [PubMed: 9225742]

Mukai H, et al. Modulation of synaptic plasticity by brain estrogen in the hippocampus. Biochim Biophys Acta. 2010; 1800:1030–44. [PubMed: 19909788]

Nelson SR, et al. Use of specific gravity in the measurement of cerebral edema. J Appl Physiol. 1971; 30:268–271. [PubMed: 5539894]

Oddo S, et al. Triple-transgenic model of Alzheimer's disease with plaques and tangles: intracellular Abeta and synaptic dysfunction. Neuron. 2003; 39:409–421. [PubMed: 12895417]

Oh KJ, et al. Staging of Alzheimer's pathology in triple transgenic mice: a light and electron microscopic analysis. Int J Alzheimers Dis. 2010:2010.

Overk CR, et al. A novel approach for long-term oral drug administration in animal research. J Neurosci Methods. 2011; 195:194–199. [PubMed: 21163304]

Overk CR, et al. Brainstem Alzheimer's-like pathology in the triple transgenic mouse model of Alzheimer's disease. Neurobiol Dis. 2009; 35:415–425. [PubMed: 19524671]

Paxinos, G.; Franklin, K. The Mouse Brain in Stereotaxic Coordinates. Academic Press; London: 2001.

Pearse G, et al. Urinary retention and cystitis associated with subcutaneous estradiol pellets in female nude mice. Toxicol Pathol. 2009; 37:227–234. [PubMed: 19181629]

Perez SE, et al. Nigrostriatal dysfunction in familial Alzheimer's disease-linked APPswe/PS1DeltaE9 transgenic mice. J Neurosci. 2005; 25:10220–10229. [PubMed: 16267229]

Pike CJ, et al. Protective actions of sex steroid hormones in Alzheimer's disease. Front Neuroendocrinol. 2009; 30:239–258. [PubMed: 19427328]

Plourde PV, et al. Arimidex: a potent and selective fourth-generation aromatase inhibitor. Breast Cancer Res Treat. 1994; 30:103–111. [PubMed: 7949201]

Rosario ER, et al. Testosterone regulation of Alzheimer-like neuropathology in male 3xTg-AD mice involves both estrogen and androgen pathways. Brain Res. 2010; 1359:281–290. [PubMed: 20807511]

Rosario ER, et al. Androgens regulate the development of neuropathology in a triple transgenic mouse model of Alzheimer's disease. J Neurosci. 2006; 26:13384–13389. [PubMed: 17182789]

Rousseeuw, P.; Leroy, A. Robust regression and outlier detection. Wiley; New York: 1987.

Rousseeuw P, Yohai V. Robust regression by means of S-estimators. Nonlinear Time Series Analysis: Lecture Notes in Statistics. 1984; 26:256–272.

unlisted. Canadian study of health and aging: study methods and prevalence of dementia. Can Med Assoc J. 1994; 150:899–913. [PubMed: 8131123]

Weiland NG, et al. Distribution and hormone regulation of estrogen receptor immunoreactive cells in the hippocampus of male and female rats. J Comp Neurol. 1997; 388:603–612. [PubMed: 9388019]

Woolley CS, et al. Naturally occurring fluctuation in dendritic spine density on adult hippocampal pyramidal neurons. J Neurosci. 1990; 10:4035–4039. [PubMed: 2269895]

Woolley CS, McEwen BS. Estradiol mediates fluctuation in hippocampal synapse density during the estrous cycle in the adult rat. J Neurosci. 1992; 12:2549–2554. [PubMed: 1613547]

Woolley CS, McEwen BS. Roles of estradiol and progesterone in regulation of hippocampal dendritic spine density during the estrous cycle in the rat. J Comp Neurol. 1993; 336:293–306. [PubMed: 8245220]

Woolley CS, et al. Estradiol increases the frequency of multiple synapse boutons in the hippocampal CA1 region of the adult female rat. J Comp Neurol. 1996; 373:108–117. [PubMed: 8876466]

Yu J, et al. An ultraperformance liquid chromatography-tandem mass spectrometry method for determination of anastrozole in human plasma and its application to a pharmacokinetic study. Biomed Chromatogr. 2011; 25:511–516. [PubMed: 20629047]

Yue X, et al. Brain estrogen deficiency accelerates Abeta plaque formation in an Alzheimer's disease animal model. Proc Natl Acad Sci U S A. 2005; 102:19198–19203. [PubMed: 16365303]

Highlights

- First detection of brain levels of anastrozole after oral administration in mice.
- Anastrozole increased $A\beta_{1\text{-}40/42}$-immunostaining in intact 3xTgAD female mice.
- Anastrozole increased number of CA1 $A\beta_{1\text{-}40/42}$ positive neurons in female mice.
- Anastrozole reduced the APP/Aβ plaque load in 9 months old female 3xTgAD mice.

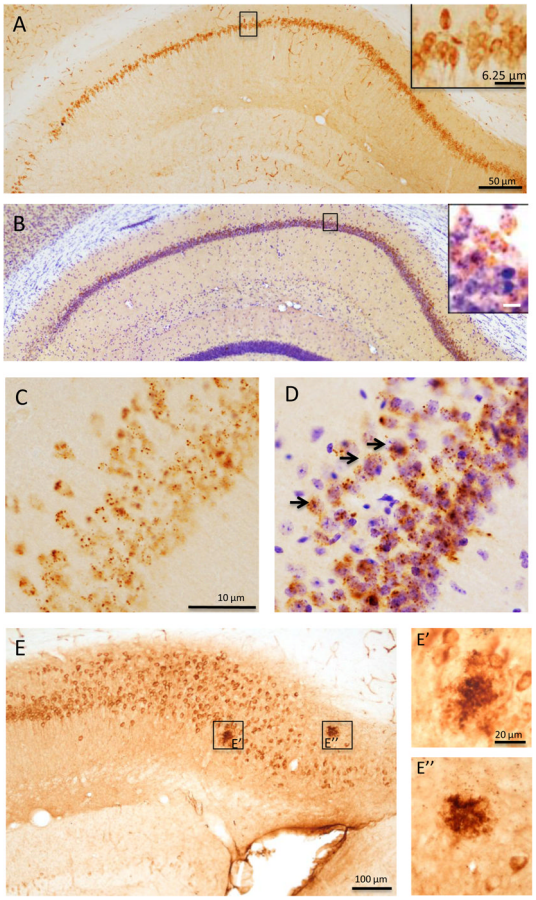

Figure 1.

Photomicrographs showing topography and morphology of APP/Aβ (A) and $Aβ_{1-40/42}$ immunoreactive profiles within the hippocampal subicular complex in 9-month old intact, control-treated female 3xTgAD mice. Tissue (A) singly immunostained for APP/Aβ (brown) and (B) a section stained for $Aβ_{1-40/42}$ and Nissl counterstained (blue) within hippocampal CA1 neurons. Insets show higher magnifications of boxed areas. Note the granular appearance of the $Aβ_{1-40/42}$ labeling shown in panels C and D (arrows). Hippocampal/subicular APP/Aβ-ir plaques (brown; E). Boxed areas are shown at a high magnification in E' and E". Scale bars in A same as for B = 50 µm, as well as the insets in A and B = 6.25 µm; C same as for D = 10 µm; E = 100 µm; and E' and E" = 20 µm.

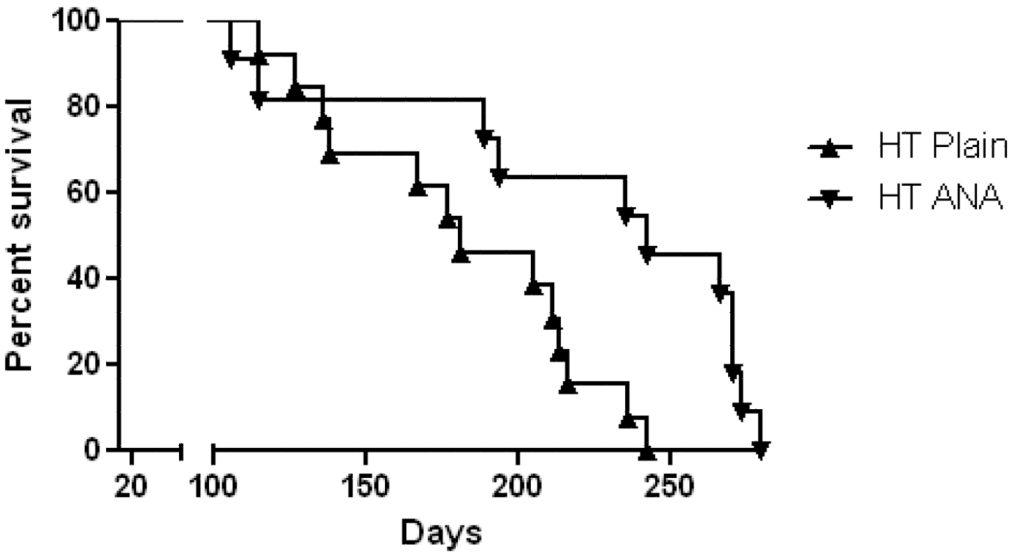

Figure 2.

Graphs showing survival rates of the HT-treated females. HT-treated females had a significant decrease in survival rate, which was prolonged by 60 days in the anastrozole (ANA)-treated group using the Kaplan-Meier estimator. All other treatment groups survived until time of sacrifice at 9 mos of age (data not shown). Figure 3. Bar graphs showing no significant difference between the groups treated with anastrozole (ANA) for either brain (open bars) or serum (hatch bars) using LC-MS (A) in 3xTgAD. Data represents mean and standard error of the mean (SEM). (B) Scatter blot showing a significant correlation between serum and brain levels of anastrozole ($p < 0.0001$; $r^2 = 0.62$).

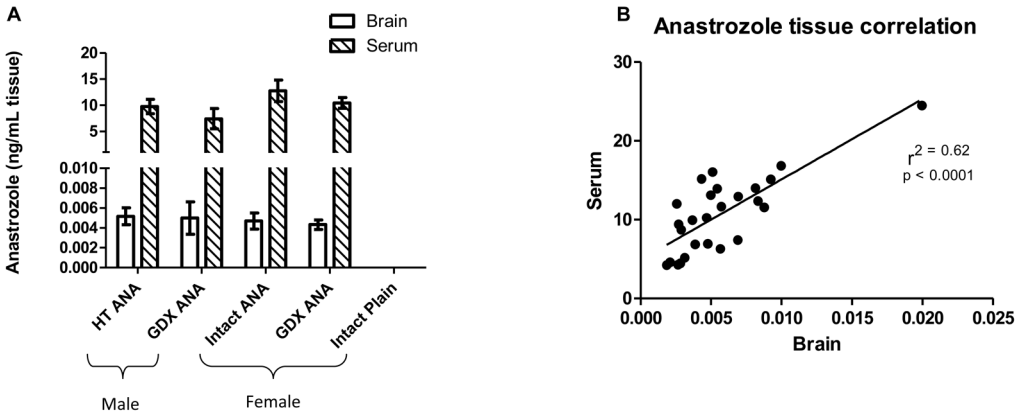

Figure 3.

Bar graphs showing no significant difference between the groups treated with anastrozole (ANA) for either brain (open bars) or serum (hatch bars) using LC-MS (A) in 3xTgAD. Data represents mean and standard error of the mean (SEM). (B) Scatter blot showing a significant correlation between serum and brain levels of anastrozole (ng/mL; $p < 0.0001$; $r^2 = 0.62$).

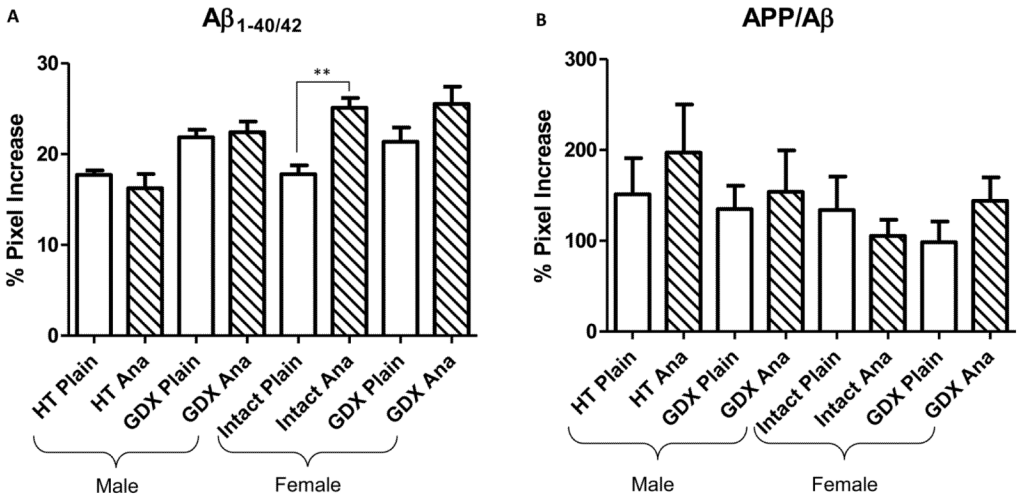

Figure 4.

Histograms showing neuronal optical density (OD) measurements of $A\beta_{1\text{-}40/42}$ (A) and APP/Aβ (B) within the CA1 hippocampal field across treatment groups. (A) $A\beta_{1\text{-}40/42}$ OD measurements were significantly greater in anastrozole (ANA) treated female intact 3xTgAD mice (hatch bars) compared to control. (B) APP/Aβ OD measures were not difference between treatment pairs. Ordinary least squares regression followed by the Holm procedure was used to adjust for multiple comparisons. Data represents predicted mean and standard error of the mean (SEM) (** p value < 0.001; open bars).

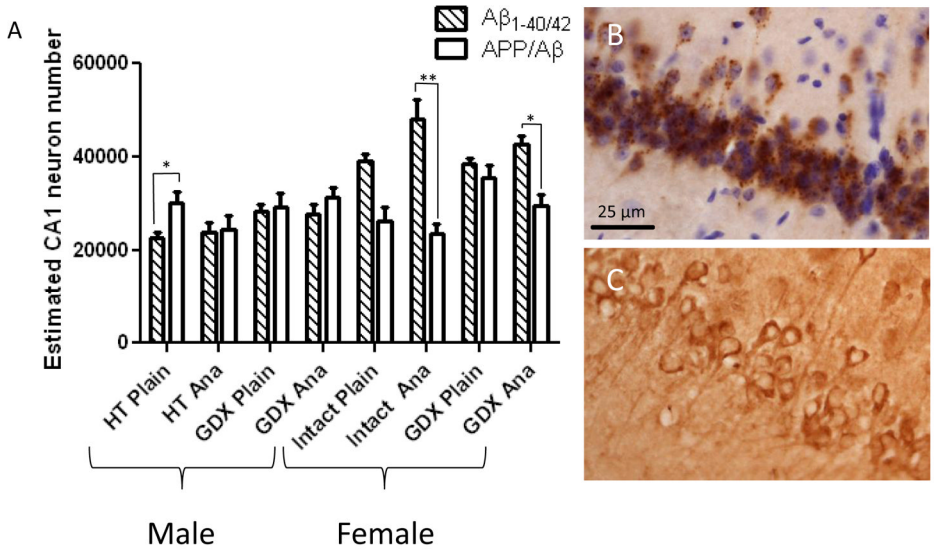

Figure 5.

Histograms showing no significant differences between CA1 neuron numbers immunoreactive for APP/Aβ (hatch bars) or $Aβ_{1-40/42}$ (open bars) between anastrozole (ANA) and control-treated pairs (A). Note the significant increase in number of $Aβ_{1-40/42}$ compared to APP/Aβ positive neurons in intact as well as ovx females treated with anastrozole. Alternatively, the number of $Aβ_{1-40/42}$ positive was decreased compared to APP/Aβ reactive neurons in HT treated male 3xTgAD mice. Representative photomicrographs of $Aβ_{1-40/42}$- (B) and APP/Aβ-ir (C). Scale bare in B is same as C, 25 μm. Poisson regression followed by the Holm procedure was applied to adjust for multiple comparisons. Data represents predicted mean and standard error of the mean (SEM) (* p value <0.01; ** p value < 0.001)

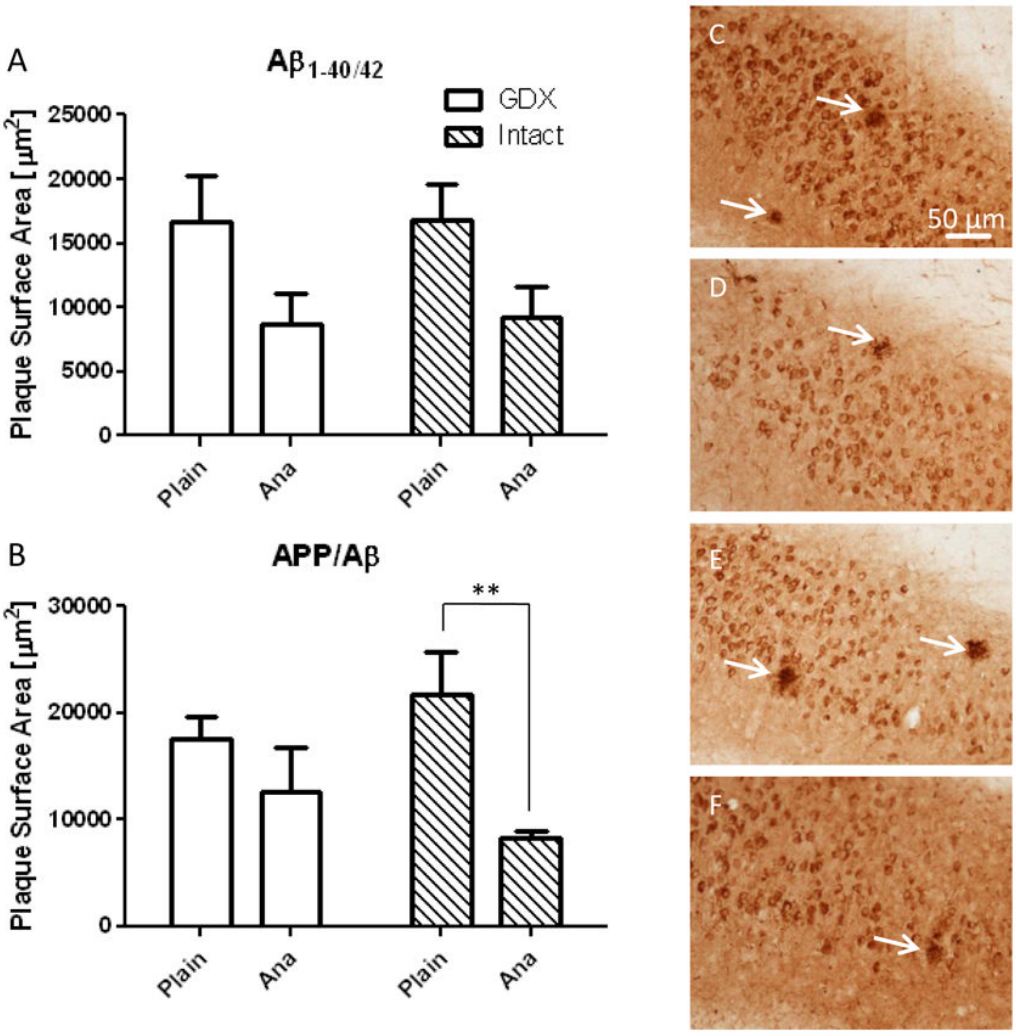

Figure 6.

Histograms showing differences in stereological estimation of plaque surface area for $A\beta_{1\text{-}40/42}$ (A) and (B) APP/Aβ in the hippocampal/subiculum region of 9-month old female 3xTgAD mice. The surface area of plaques visualized by APP/Aβ was significantly decreased in intact mice treated with anastrozole (ANA). Representative photomicrographs of APP/Aβ-positive plaques (arrows) in GDX plain (C), GDX ANA (D), intact plain (E), and intact ANA (F) treated groups. Scale bar in C, 50 μm, applies to D-F. The minimum scale estimator followed by the Holm procedure was used to adjust for multiple comparisons. Data represents predicted mean and standard error of the mean (SEM) (* $p < 0.01$).

Table 1

Treatment groups.

Sex	Surgery group	Treatment group	Number (samples collected early)
Female	GDX	Plain	8
Female	GDX	ANA	8
Female	GDX + HT	Plain	(8)
Female	GDX + HT	ANA	(6)
Female	Intact	Plain	8
Female	Intact	ANA	8
Male	GDX	Plain	8
Male	GDX	ANA	8
Male	GDX + HT	Plain	8
Male	GDX + HT	ANA	8